The Advanced Microwave Radiometer – Climate Quality (AMR-C) Instrument for Sentinel-6

Jenna L. Kloosterman[1,*], Shannon Brown[1], Timothy Koch[1], Nho Vo[1], Fabien Nicaise[1], Erich Schlecht[1], Matthew Bloom[1], Lance Milligan[1], K. Scott Tripp[1], Pekka Kangaslahti[1], Isaac Ramos[1], Shannon Statham[1], Anders Skalare[1], Richard Cofield[1], Frank Maiwald[1]
[1]*Jet Propulsion Laboratory, California Institute of Technology, 91106 Pasadena, CA, USA*
*Contact: Jenna.L.Kloosterman@jpl.nasa.gov

Abstract— **The Advanced Microwave Radiometer – Climate Quality (AMR-C) is designed to measure the path delay due to atmospheric water vapor along Sentinel-6 altimeter path over one decade. The AMR-C receiver is based on heritage from previous AMR instruments with the addition of a THz-frequency radiometer, the High Resolution Microwave Radiometer (HRMR), for improved coastal zone accuracy and a Supplemental Calibration System (SCS) to meet level 3 requirements that the path delay error due to the altimeter-derived sea surface height be less at 0.8 cm and the path delay stability be maintained to 0.7 mm averaged over a 1-year time period.**

I. INTRODUCTION

The Sentinel-6 Mission will provide continuity to ocean topography measurements made from previous missions TOPEX-Poseidon (launched in 1992) [1], Jason-1 (2001) [2], OSTM/Jason-2 (2008) [3], and Jason-3 (2016) [4]. These measurements are important in determining ocean circulation, climate change, and sea level rise year-over-year. The results of these missions show a clear global mean sea rise of ~3+ mm/yr, shown in Figure 1 [5]. The Sentinel-6 mission consists of two satellites to be launched approximately 5 years apart. Each satellite is designed for a 5.5-year mission to extend measurements for at least another decade.

Sentinel-6 consists mainly of two instruments: an altimeter and a radiometer. These two instruments in combination will enable the mission to achieve its level 1 requirement to measure year-over-year global mean sea level stability to within 1 mm. These requirements flow to the payload level 3 requirements that the path delay error due to altimeter-derived sea surface height will be 0.8 cm. The level 3 requirements flow to the level 4 instrument requirements, which are derived from a global path delay retrieval algorithm. The level 4 instrument requirements are that microwave brightness temperature error will be less than 0.65 K at a 1 Hz sample rate and the radiometer brightness temperature will be stable to +/- 0.1K over a one year period.

The focus of this paper will be the radiometer instrument, the Advanced Microwave Radiometer – Climate Quality (AMR-C), which has completed the instrument preliminary design review (PDR) and is now finalizing the flight designs.

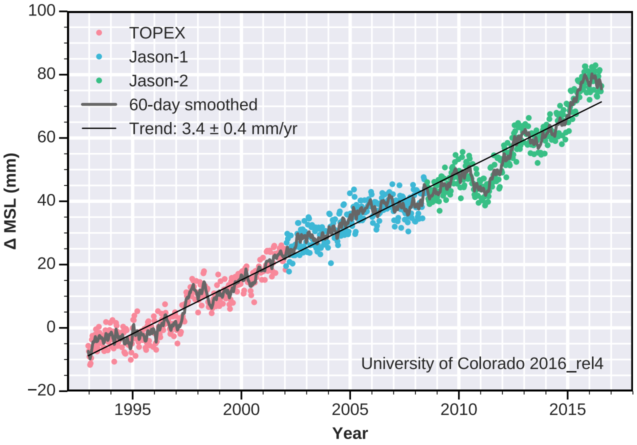

Figure 1. Global mean sea level rise from TOPEX, Jason-1, and Jason-2 after seasonal variations are removed [5]. The trend is a rise of ~3 mm/yr.

II. INSTRUMENT DESCRIPTION

The AMR-C receiver is based on heritage from the previous missions with addition of a High Resolution Microwave Radiometer (HRMR) [6] and a Supplemental Calibration System (SCS). The radiometer channels at 18.7 GHz, 23.8 GHz, and 34.0 GHz are inherited from previous AMRs and constitute the radio frequency subassembly (RFA). The 18.7 GHz channel estimates ocean surface components in observed brightness temperature, the 23.8 GHz channel estimates water vapor, and the 34.0 GHz channel estimates cloud liquid. HRMR consists of bands at 90 GHz, 130 GHz, and 168 GHz. The SCS is an additional calibration system in order to meet the level 3 payload requirement of long term radiometric stability. In addition to the RFA, HRMR, and SCS subassemblies, the AMR-C instrument also contains a parabolic mirror in the Reflector Subassembly (RSA), and the Electronics Unit (EU) in the Electronics Subassembly (ESA). An AMR-C instrument model with all five subassemblies is shown in Figure 2.

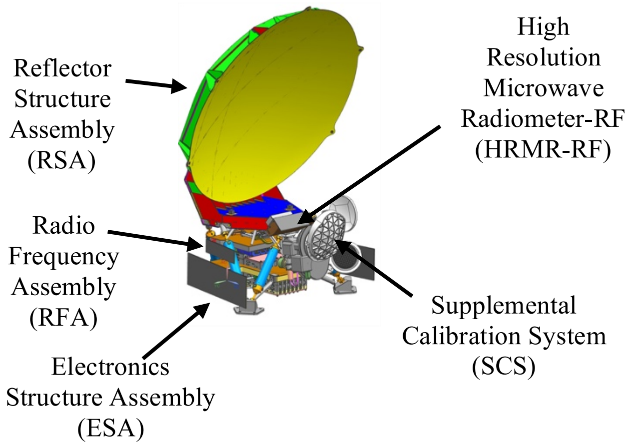

Figure 2. AMR-C instrument model with each of the major subsystems.

A block diagram of the AMR-C instrument is shown in Figure 3. HRMR sits at the focus of the primary reflector and the lower frequency channels in the RFA are offset. There are two identical lower frequency radiometer units in the AMR-C system, a nominal unit (H-polarization) and a redundant unit (V-polarization) shown in green. All three of these receivers have a separate EU containing the Power Converter Unit (PCU), a Data Acquisition and Control Unit (DAC), and a Housekeeping Unit (HKU). The DACs of the AMR-H and AMR-V units are crossed-strapped to the SCS shown in purple, which has fully redundant Control Mechanism Interface Electronics (CMIE) units, both of which can control either or both motors in the Standard Dual Drive Actuator (SDDA). Please note that cross-strapping in Figure 3 is only shown for the EU-H unit to reduce clutter in the figure. HRMR is in turquoise.

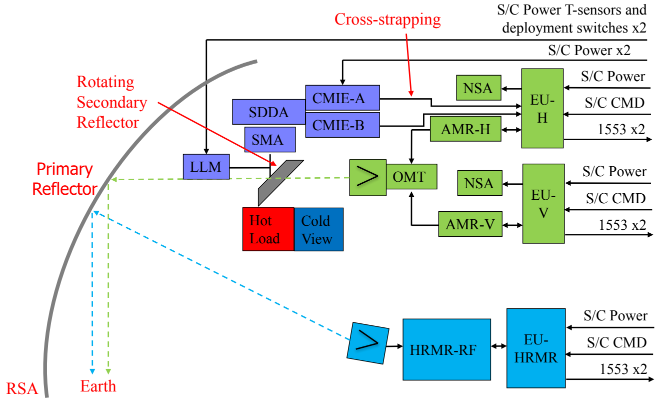

Figure 3. AMR-C block diagram. Each subsystem is color-coded (with its EU unit).

III. INSTRUMENT DESIGN

A. AMR-H and AMR-V Receiver Design

Signal is relayed to the receiver through a circular feed horn. The signal is split by the Ortho-mode Transducer (OMT) into H and V units, nominal and redundant, respectively, although the polarization is arbitrary. The redundant unit will be used as a cold spare. From the OMT a diplexer divides the signal into 18/24 GHz and 34 GHz channels and the 18/24 GHz channel is then spilt into separate 18 and 24 GHz channels. A detector diode along with an ADC converts the signal to a digital signal, which is then relayed to the spacecraft and transmitted to the ground. A model of the receivers is shown in Figure 4 and an internal block diagram is shown in Figure 5. In operation, a Dicke switch at the receiver waveguide output toggles between the antenna signal and 50 Ω load for a differential measurement.

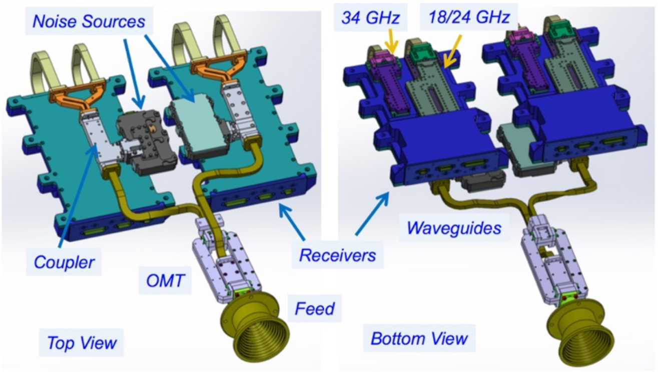

Figure 4. Top and bottom views of the AMR receivers for 18/24 and 34 GHz.

TABLE 1. LEVEL 6 AMR INSTRUMENT REQUIREMENTS.

Parameter	**Requirement**		
Input Return Loss (over channel passbands)	≥ 15 dB		
Dicke Switch Isolation	≥ 30 dB		
Channel Center Frequency	18.7 GHz	23.8 GHz	34.0 GHz
Center Frequency Tolerance	±50 MHz	±100 MHz	± 100 MHz
Center Frequency Knowledge	± 20 MHz	± 20 MHz	± 50 MHz
Channel Noise Bandwidth	200 MHz	400 MHz	700 MHz
Noise Bandwidth Tolerance	± 50 MHz	± 100 MHz	± 150 MHz
Passband Ripple	± 1 dB max	± 1 dB max	± 1 dB max
Stopband Rejection	> 50 dB	> 50 dB	> 50 dB
System Noise Figure	≤ 6.2 dB	≤ 6.5 dB	≤ 6.6 dB
System Gain/Temperature Coefficient	≤ 0.2 dB/℃	≤ 0.2 dB/℃	≤ 0.2 dB/℃
Post-detector Circuit Video (3 dB) Bandwidth	≥ 75 kHz	≥ 75 kHz	≥ 75 kHz
Backend Noise (relative to radiometric noise)	≤ 1/3	≤ 1/3	≤ 1/3
Input Dynamic Range	2.7 to 750 K		
Digitizer Sampling Rate	≥ 200 ksps		

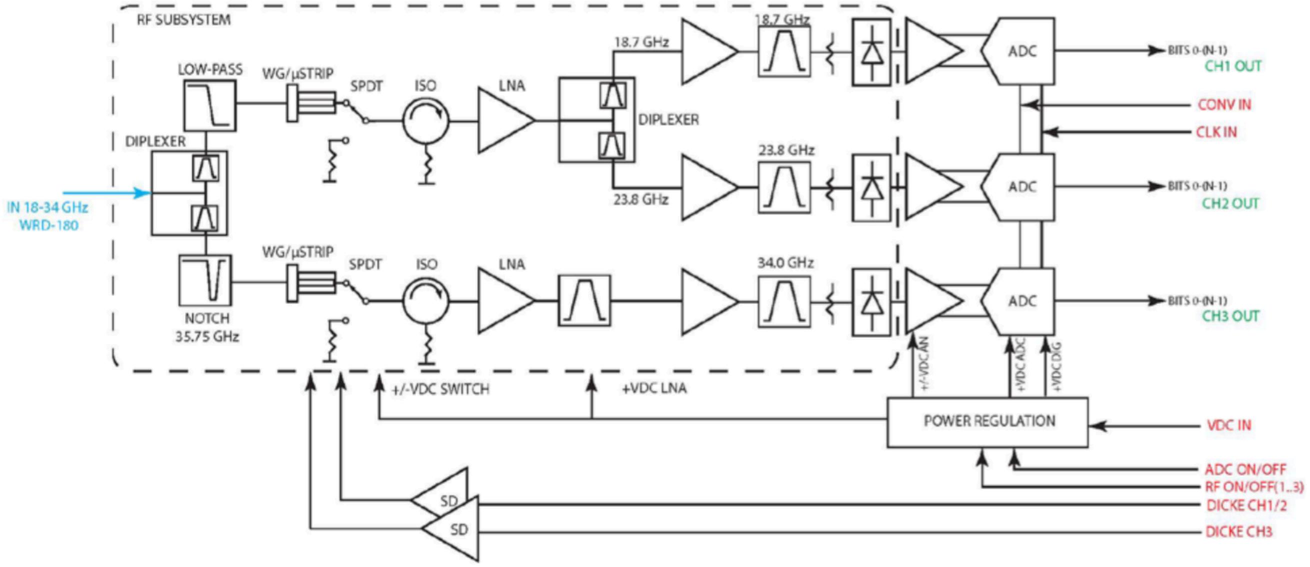

Figure 5. AMR receiver block diagram.

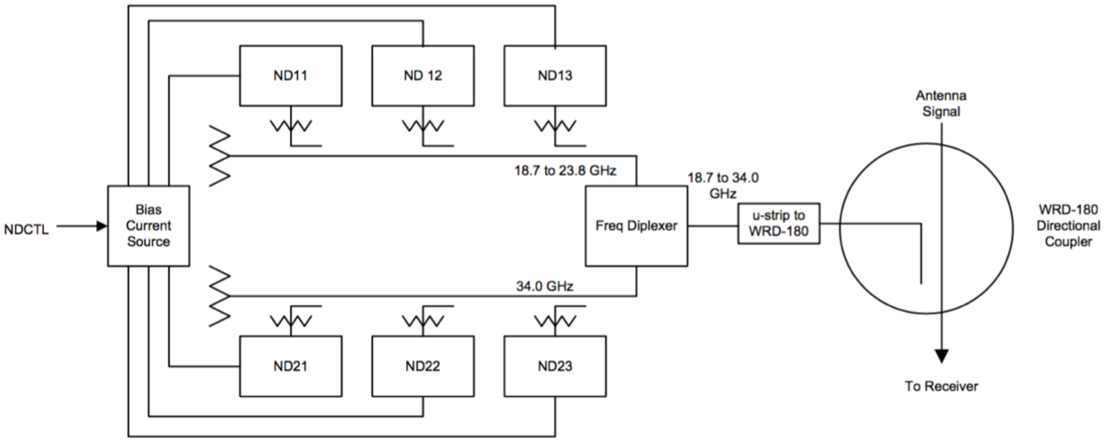

Figure 6. The AMR noise source block diagram.

A fully characterized noise source at the input of each receiver is used for internal gain stability calibration. Each noise source contains 3 sets of redundant diodes that can be used separately or together. A block diagram for the noise source is shown in Figure 6. The noise signals are coupled at the receiver input using a directional coupler.

The level 6 receiver requirements flow from the level 4 instrument requirements. These requirements are summarized in TABLE 1.

B. HRMR Receiver Design

Previous AMRs were limited to a 25 km diameter footprint on the ocean. In order to provide higher spatial resolution to improve the coastal zone measurement accuracy to a 3-5 km diameter footprint, a THz radiometer, HRMR, has been added to the AMR-C instrument. HRMR includes receiver bands at 90 GHz, 130 GHz, and 168 GHz and is based on radiometers designed for airborne and cubesat missions, the High-frequency Airborne Microwave and Millimeter-wave Radiometer (HAMMR) [7], and the Temporal Experiment for Storms and Tropical Systems (TEMPEST) [8], respectively. HRMR has been designed to attach to three mounting points at the focus of the RSA to minimize AMR beam blockage. The feedhorn and millimeter wave modules will be assembled and delivered on a radiatively-cooled plate, which will be enclosed for better thermal shielding.

HRMR will interface with EU hardware identical to the AMR units through its digitizer driver unit (DDU). This receiver utilizes low noise, high gain Indium Phosphide (InP) MMICs [9] to amplify incoming signal in order to detect it. Like the AMRs, HRMR signal is relayed through a feedhorn into diode detectors for each frequency. The calibration noise source is integrated in the multi-chip module (MCM). It has two noise diodes and directional couplers to provide stable calibration references. Additional calibration and stability is provided by the integrated Dicke switch that toggles between the antenna and reference load at 2 kHz rate to reduce NEDT, see Figure 13. A model of the HRMR receivers is shown in Figure 7 and design parameters are shown in TABLE 2.

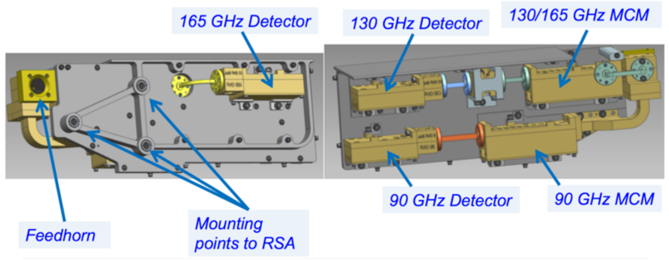

Figure 7. Top and bottom views of the HRMR receiver.

TABLE 2. HRMR RECEIVER DESIGN PARAMETERS

Parameter	**Requirement**		
Channel Center Frequency	90 GHz	130 GHz	168 GHz
Center Frequency Tolerance	±5 GHz	±5 GHz	± 5 GHz
Minimum Bandwidth	5 GHz	5 GHz	5 GHz
Noise Temperature	2000 K	2500 K	3500 K
Brightness Temperature Sensitivity	0.2 K	0.2 K	0.2 K
Deviation from White Noise Level Over 60 secs	< 0.2 K	< 0.2 K	< 0.2 K

C. The SCS

Due to long term fluctuations seen in the noise source from the Jason-3 mission [4] a Supplemental Calibration System (SCS) has been included on AMR-C. This subsystem is designed to turn the secondary mirror every 5-10 days so that the AMR receivers look at a warm load at ambient temperature (~200 K) and a cold load (cold sky, ~3 K), shown in Figure 8. As shown in Figure 3, the SCS only calibrates the AMR receivers, not HRMR, whose signal path is instead at the focus of the primary. These calibrations will be done over land in order to maximize observation times over the ocean.

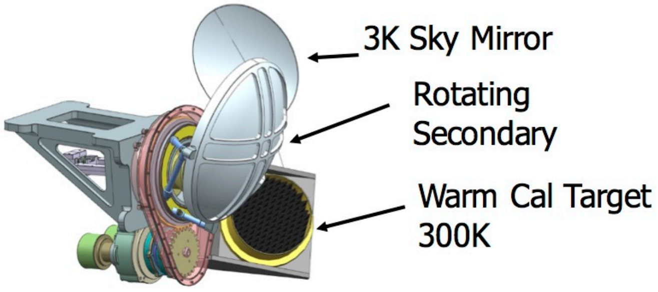

Figure 8. The SCS, which rotates a secondary mirror to look at ambient and cold calibration targets.

The SCS is driven by an SDDA motor, which is a block redundant, single fault tolerant mechanical/electronic assembly that provides a rotary output with fully characterized torque, speed, and current relationships. The gearbox couples dual spur gears for the first stage with dual harmonic gears in the final stage. The redundancy in the SDDA means that no single mechanism failure within the assembly will prevent the output from rotating. The SDDA power is supplied separately from the rest of the instrument. The mechanism control is cross-strapped to both the H and V flight computers. During launch the secondary mirror is held in place by the Launch Lock Mechanism (LLM).

IV. Initial Results

A. Thermal Modeling

The AMR-C instrument will have a PID-controlled thermal loop run by the spacecraft. The preliminary thermal design was simulated using a P-regulator and modeling shows that the receiver will meet its thermal requirements detailed below. The thermal analysis was done for three different cases: a hot winter, a hot summer, and a cold summer. Results are shown for several simulations lasting the duration of one orbit, which is 112 minutes long. Figure 9 models the AMR-H receiver thermal stability over one orbit showing that it can be kept to within ~0.04 °C/min. Similarly, Figure 10 shows the modeled thermal stability for HRMR. HRMR has no requirement, but the goal for this receiver is ≤ 0.1 °C of variation over an orbit. Peaks and minimums in these models are a result of the satellite's orbit as it transitions in and out of the sun. In Figure 11, models show the thermal variation within the AMR-H receiver will be ± 2.5 °C. Figure 12 shows the thermal variations between the feed horn assembly (FHA) and the AMR-H receiver. The requirement is these thermal variations not exceed 10 °C and models show that this difference is well within the model's margin.

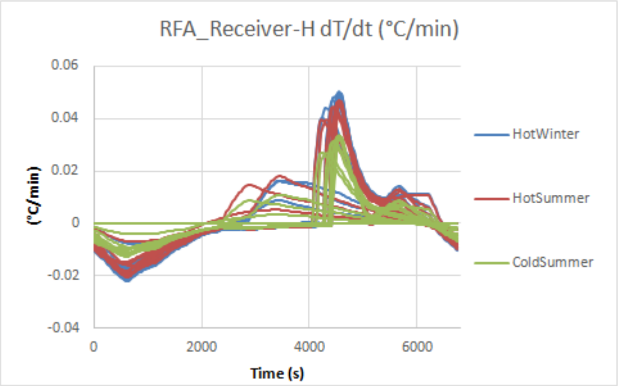

Figure 9. AMR-H receiver thermal stability can be kept to less than 0.04 °C/min during an orbit.

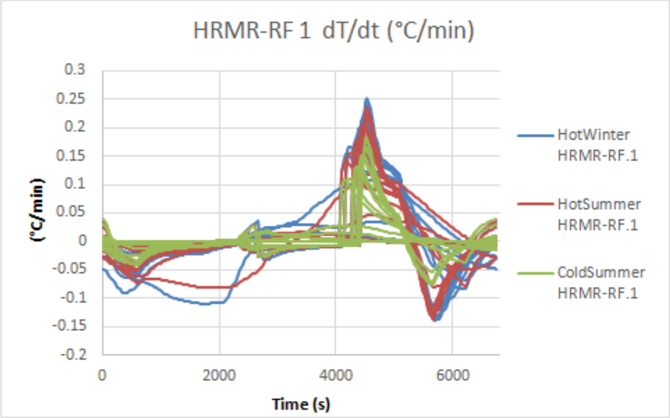

Figure 10. HRMR thermal stability models. The goal is ≤ 0.1 °C

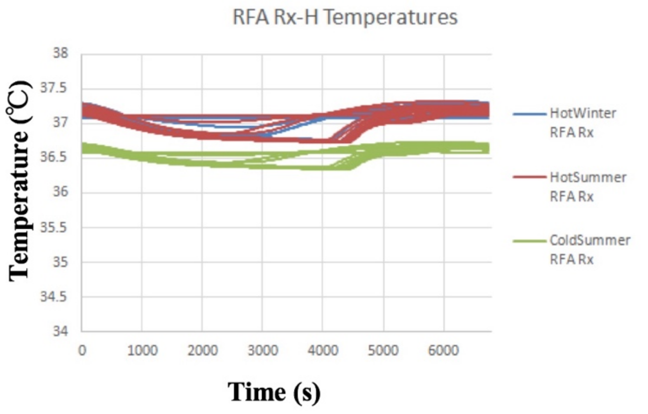

Figure 11. The AMR-H temperature range is ± 2.5 °C within the receiver.

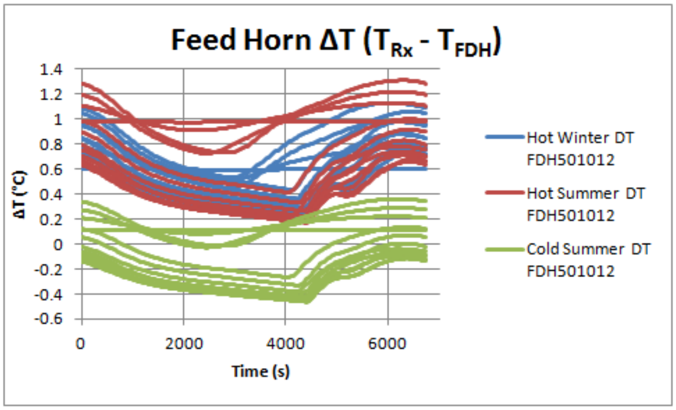

Figure 12. The thermal variations between the feed horn and the receiver over one orbit.

B. HRMR Prototype

The HRMR 90 GHz prototype's measured noise temperature is ~500 K. The noise equivalent differential measurement (NEDT) was measured for both 90 and 160 GHz. The NEDT is a measure of sensitivity that determines the threshold for the minimum differential temperature that the system can detect. This measurement is taken by looking at the difference between the receiver looking at a blackbody radiator and a 50 Ω reference load using a Dicke switch. The results of the NEDT measurements for 90 and 160 GHz prototype receivers are presented in Figure 13. The NEDT at 90 GHz is in green and the NEDT at 160 GHz is in blue. At the Dicke switch frequency of 2 kHz, the NEDTs ~0.1 K, which provides a 50% margin on the sensitivity requirement.

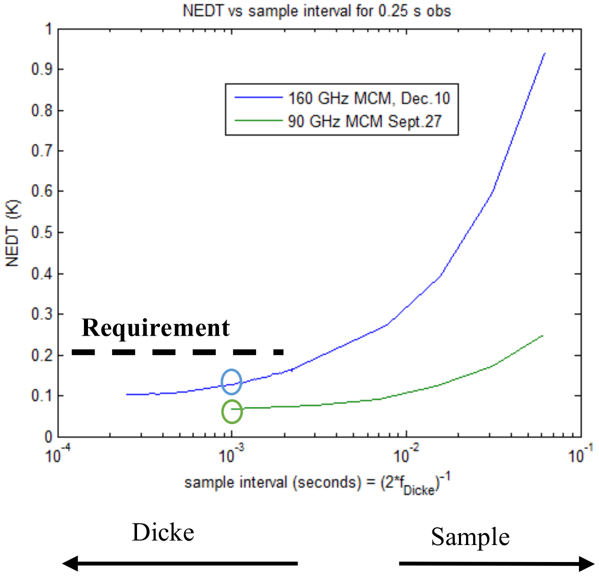

Figure 13. HRMR NEDT measurements for prototype HRMR receivers at 90 and 160 GHz.

Further measurements made on the prototype indicate that the power and mass are within the margins of their allotted budgets. These results are presented in TABLE 3.

TABLE 3. HRMR PROTOTYPE SPECIFICATIONS

Requirement	Prototype Measurement	Requirement	Margin
Power (W)	2.84	3.2	11%
Mass (kg)	1.98	2.2	10%
NEDT (K)	<0.1	0.2	50%
Deviation from white noise over 60 s [K]	0.05	<0.2	75%

V. CURRENT STATUS AND FUTURE WORK

The AMR-C team plans to deliver two flight instruments, one for each mission ~5 years apart. The instrument has passed the preliminary design review (PDR) and Phase C has begun. Hardware testing will begin in the summer of 2017 and the critical design review (CDR) will be in the fall of 2017. Instrument I&T for the first flight module will start in the Spring of 2018 for delivery to payload I&T in early 2019. Instrument I&T for the second flight module will begin in early 2019 after the delivery of the first flight module, and begin payload I&T in fall 2019. Sentinel-6 is expected to launch in 2020.

ACKNOWLEDGMENT

The research was carried out at the Jet Propulsion Laboratory, California Institute of Technology, under a contract with the National Aeronautics and Space Administration.

REFERENCES

[1] C. S. Ruf, S. J. Kienhm, and M. A. Janssen, "TOPEX/Poseidon Microwave Radiometer (TMR). I. Instrument description and antenna temperature calibration," in *IEEE Transactions on Geoscience and Remote sensing*, vol. 33, no. 1, pp. 125-137, Jan. 1995.

[2] Y. Ménard, L. L. Fu, P. Escudier, F. Parisot, J. Perbos, P. Vincent, S. Desai, B. Hanes, and G. Kunstmann, "The Jason-1 mission special issue: Jason-1 calibration/validation," in *Marine Geodesy,* vol. 26, no. 3-4, pp. 131-146, Jul. 2003.

[3] J. Lambin, R. Morrow, L. L. Fu, J. K. Willis, H. Bonekamp, J. Lillibridge, J. Perbos, G. Zaouche, P. Vaze, W. Bonnoura, F. Parisot, E. Thouvenot, S. Coutin-Faye, E. Lindstrom, and M. Mignogno, "The OSTM/Jason-2 mission," in *Marine Geodesy,* vol. 33, no. S1, pp. 4-25, Aug. 2010.

[4] F. Maiwald, O. Montes, S. Padmanabhan, D. Michaels, A. Kitiyakara, R. Jarnot, S. T. Brown, D. Dawson, A. Wu, W. Hatch, P. Stek, T. Gaier, "Reliable and Stable Radiometers for Jason-3," in *IEEE Journal of Selected Topics in Applied Earth Observations and Remote Sensing,* vol. 9, no. 6, pp. 2754-2762, June 2016.

[5] R. S. Nerem, D. P. Chambers, C. Choe, and G. T. Mitchumm, "Estimating mean sea level change from the TOPEX and Jason altimeter missions." in *Marine Geodesy,* vol. 33, no. S1, pp. 435-446, Aug. 2010.

[6] P. Kangaslahti, E. Schlecht, J. Jiang, W. R. Deal, A. Zamora, K. Leong, S. C. Reising, X. Bosch, and M. Ogut, "CubeSat scale receivers for measurement of ice in clouds," in *2016 14th Specialist Meeting on Microwave Radiometry and Remote Sensing of the Environment (MicroRad),* Espoo, 2016, pp. 42-47.

[7] S. Reising, P. Kangaslahti, A. B. Tanner, S. Padmanabhan, O. Montes, and C. Parashare, "Demonstration of High-frequency Airborne Microwave and Millimeter-Wave Radiometer (HAMMR) to Improve Spatial Resolution of Wet-Tropospheric Path Delay Measurements for Coastal and Inland Water Altimetry," in *NASA Earth Science Technology Forum 2014*.

[8] S. C. Reising, T. C. Gaier, C. D. Kummerow, V. Chandrasekar, S. T. Brown, S. Padmanabhan, B. H. Lim, S. C. van den Heveer, T. S. L'Ecuyer, C. S. Ruf, Z. S. Haddad, Z. J. Luo, S. J. Munchak, G. Berg, T. C. Koch, and S. A. Boukabara, "Overview of Temporal Experiment for Storms and Tropical Systems (TEMPEST) CubeSat constellation mission." In *2015 IEEE MTT-S International Microwave Symposium (IMS)*, 2015, pp. 1-4.

[9] X. Mei W. Yoshida, M. Lange, J. Lee, J. Zhou, P.-H. Liu, K. Leong, A. Zamora, J. Padilla, S. Sarkozy, R. Lai, and W. R. Deal, "First Demonstration of Amplification at 1 THz Using 25-nm InP High Electron Mobility Transistor Process," in *IEEE Electron Device Letters*, vol. 36, no. 4, pp. 327-329, April 2015.